axioms

MDPI

Article

Approximate and Parametric Solutions to SIR Epidemic Model

Lazhar Bougoffa [1,*], Smail Bougouffa [2] and Ammar Khanfer [3]

[1] Department of Mathematics, Faculty of Science, Imam Mohammad Ibn Saud Islamic University (IMSIU), Riyadh 11623, Saudi Arabia
[2] Department of Physics, Faculty of Science, Imam Mohammad Ibn Saud Islamic University (IMSIU), Riyadh 11623, Saudi Arabia; sbougouffa@imamu.edu.sa
[3] Department of Mathematics and Sciences, Prince Sultan University, Riyadh 11586, Saudi Arabia; akhanfer@psu.edu.sa
* Correspondence: lbbougoffa@imamu.edu.sa

Abstract: This article provides a detailed exploration of the SIR epidemic model, starting with its meticulous formulation. The study employs a novel approach called the upper and lower bounds technique to approximate the solution to the SIR model, providing insights into the dynamic interplay between susceptible S, infected I, and recovered R populations. A new parametric solution to this model has been presented. Applying the Adomian decomposition method (ADM) allows for the attaining of highly accurate approximate solutions in the context of the SIR epidemic model. To validate the accuracy and robustness of the proposed approach, a numerical exploration is conducted, considering a diverse range of experimental parameters. This numerical analysis provides valuable insights into the sensitivity and responsiveness of the SIR epidemic model under varying conditions, contributing to the broader understanding of infectious disease dynamics. The interplay between theoretical formulation and numerical exploration establishes a comprehensive framework for studying the SIR model, with implications for refining our ability to predict and manage the spread of infectious diseases.

Keywords: SIR epidemic model; upper bound of solution; lower bound of solution; solution in parametric form; Adomian decomposition method

MSC: 39A27; 65L10; 34L15; 49M27

Citation: Bougoffa, L.; Bougouffa, S.; Khanfer, A. Approximate and Parametric Solutions to SIR Epidemic Model. *Axioms* **2024**, *13*, 201. https://doi.org/10.3390/axioms13030201

Academic Editors: Cheng-Cheng Zhu, Patricia J. Y. Wong and Hari Mohan Srivastava

Received: 25 January 2024
Revised: 25 February 2024
Accepted: 14 March 2024
Published: 16 March 2024

1. Introduction

The SIR epidemic model provides a rigorous framework for understanding the temporal evolution of a population's susceptibility S, infection I, and recovery R to time t. This model is described by a set of non-linear ordinary differential equations, as presented in Equation (1) [1,2]:

$$\begin{cases} \frac{dS}{dt} &= -rSI, \\ \frac{dI}{dt} &= rSI - \alpha I. \end{cases} \tag{1}$$

These equations encapsulate the dynamics of S, I, and R populations, with the initial conditions outlined in Equation (2):

$$S(0) = S_0,\ I(0) = I_0, \tag{2}$$

where $r, \alpha, S(0)$ and $I(0)$ are non-negative constant parameters. The equation describing the behavior of R evolves from the infected population I, expressed as

$$R(t) = \alpha \int_0^t I(\tau) d\tau. \tag{3}$$

The SIR (Susceptible-Infectious-Removed) model is a fundamental and significant epidemiological model due to its simplicity, clarity, and historical importance. Although more complex and modern models [3–8], have been developed to address specific small differences in infectious disease dynamics, the SIR model remains valuable. The choice of model depends on analysis objectives and the level of detail needed.

A substantial body of literature has been dedicated to numerical methods for solving these equations, such as the homotopy analysis method (HAM) [9]. Recently, in [10], the authors explored this coupled non-linear system and introduced an approximate solution through asymptotic approximants.

This paper is devoted to finding the new upper and lower bounds of solutions to this SIR epidemic model in explicit forms. Further, finding lower and upper bounds for solutions to differential equations is an important mathematical and analytical tool. It can provide insights, validation, and practical benefits in understanding and modeling various physical and engineering systems. These bounds help to characterize the behavior and limitations of the system under study.

It is often challenging, if possible, to find explicit solutions to some systems. However, converting such a system to an equivalent second-order nonlinear differential equation can help in finding solutions in parametric form. As a result, a new solution in parametric form can be provided.

Overall, the Adomian decomposition method (ADM) [11–23] is a powerful analytical method for approximating solutions to the SIR epidemic model, contributing significantly to understanding disease dynamics and informing public health strategies. The ADM provides an analytical framework that offers closed-form or series solutions, which helps in obtaining analytical expressions for the SIR model's behavior over time. Moreover, the ADM allows for the handling of nonlinear differential equations, enabling the study of complex epidemic models that often exhibit nonlinear dynamics and providing a more realistic representation of disease spread. The ADM can yield accurate solutions, particularly for problems with known or expected smooth solutions, contributing to a precise understanding of epidemic behavior and dynamics. Therefore, we use the ADM to find excellent approximation solutions for the SIR epidemic model concerning real scenarios. Results obtained from the Adomian method are compared with numerical solutions, providing validation and a better understanding of the model's behavior.

2. Solutions to System (1)–(3)

We first begin by converting system (1) and (2) to an equivalent system through the following transformations:

$$S = e^u,\ I = e^v. \tag{4}$$

Substituting (4) into (1) and (2), we obtain

$$\begin{cases} \frac{du}{dt} &= -re^v, \\ \frac{dv}{dt} &= re^u - \alpha, \\ u(0) &= \ln S_0,\ v(0) = \ln I_0. \end{cases} \tag{5}$$

2.1. Upper and Lower Bounds of Solutions

The following fundamental lemma is an important tool in finding the upper and lower bounds of system solutions (1)–(3).

Lemma 1. *The following system,*

$$\begin{cases} \frac{du}{dt} &= -re^v, \\ \frac{dv}{dt} &= re^u - \alpha \end{cases} \tag{6}$$

can be converted into an equivalent first-order nonlinear equation in u,

$$\frac{du}{dt} = re^u - \alpha u + c_1, \tag{7}$$

where c_1 is a constant of integration.

Proof. Differentiating the first equation of Equation (6) with respect to t, we obtain

$$\frac{d^2u}{dt^2} = -r\frac{dv}{dt}e^v. \tag{8}$$

We eliminate $\frac{dv}{dt}$ and e^v from (8) by using the first and second equations of Equation (6), and we obtain

$$\frac{d^2u}{dt^2} = r\frac{du}{dt}e^u - \alpha\frac{du}{dt}. \tag{9}$$

Integrating Equation (9) with respect to t, we obtain Equation (7), which is a first-order nonlinear equation in the unknown function u.

Conversely, we can reduce Equation (7) to Equation (6) by setting the transformation $\frac{du}{dt} = -re^v$; thus, Equation (9) can be decoupled into

$$\begin{cases} \frac{du}{dt} &= -re^v, \\ -r\frac{dv}{dt}e^v &= -r^2e^ve^u + \alpha re^v, \end{cases} \tag{10}$$

which is indeed (6). □

We now rewrite Equation (7) in the form

$$\frac{du}{dt} = f(t,u), \tag{11}$$

where $f(t,u) = re^u - \alpha u + c_1$ with $u(0) = \ln S_0$.

Now, using the well-known exponential inequality $e^u \geq 1 + u,\ u \in \mathbb{R}$, we get

$$f(t,u) \geq c_1 + r + (r-\alpha)u, \tag{12}$$

that is,

$$f(t,u) \geq g(t,u), \tag{13}$$

where $g(t,u) = c_1 + r + (r-\alpha)u$.

For comparison purposes, we have the following initial-value problem for the linear equation:

$$\frac{dw}{dt} = c_1 + r + (r-\alpha)w,\ w(0) = u(0) = \ln S_0. \tag{14}$$

The solution to w is then easy:

$$w(t) = \left(\ln S_0 - \frac{c_1 + r}{\alpha - r}\right)e^{(r-\alpha)t} + \frac{c_1 + r}{\alpha - r}. \tag{15}$$

Since $g(t,w)$ is continuous in t and w and Lipschitz in w, we can apply the comparison theorem to Equation (11) with $u(0) = \ln S_0$ to get

$$u \geq w,\ t \geq 0. \tag{16}$$

Consequently,

$$S \geq e^{w},\ t \geq 0, \tag{17}$$

which is the lower bound of S.

To now find the lower bound of I, from the system (5), we take the second equation:

$$\frac{dv}{dt} = re^{u} - \alpha. \tag{18}$$

In view of this and since $e^{u} \geq e^{w}$, we obtain

$$\frac{dv}{dt} \geq re^{w} - \alpha. \tag{19}$$

A simple integration from 0 to t leads to

$$v \geq r\int_{0}^{t} e^{w(\tau)}d\tau - \alpha t + \ln I_0. \tag{20}$$

Hence,

$$e^{v} \geq e^{\left(r\int_{0}^{t} e^{w(\tau)}d\tau - \alpha t + \ln I_0\right)}. \tag{21}$$

Consequently,

$$I \geq I_0 e^{\left(r\int_{0}^{t} e^{w(\tau)}d\tau - \alpha t\right)}. \tag{22}$$

It remains, therefore, only to find the upper bounds of S and I. In finding them, we shall make use of Equations (1). Indeed, from the first equation of Equations (1),

$$\frac{dS}{dt} = -rSI \tag{23}$$

and in view of (22), we obtain

$$\frac{dS}{dt} \leq -rI_0 e^{\left(r\int_{0}^{t} e^{w(\tau)}d\tau - \alpha t\right)} S. \tag{24}$$

It follows that

$$\ln S \leq -rI_0 \int_{0}^{t} e^{\left(r\int_{0}^{\xi} e^{w(\tau)}d\tau - \alpha\xi\right)}d\xi + \ln S_0, \tag{25}$$

or

$$S \leq S_0 e^{-rI_0\int_{0}^{t} e^{\left(r\int_{0}^{\xi} e^{w(\tau)}d\tau - \alpha\xi\right)}d\xi}. \tag{26}$$

Similarly, from the second equation of Equation (1):

$$\frac{dI}{dt} = rSI - \alpha I \tag{27}$$

and in view of (26), we obtain

$$\frac{dI}{dt} \leq \left[rS_0 e^{-rI_0\int_{0}^{t} e^{\left(r\int_{0}^{\xi} e^{w(\tau)}d\tau - \alpha\xi\right)}d\xi} - \alpha\right] I. \tag{28}$$

A simple integration again from 0 to t gives us

$$\ln I \leq rS_0 \int_0^t Z(\tau)d\tau - \alpha t + \ln I_0, \tag{29}$$

or

$$I \leq I_0 e^{-\alpha t} e^{rS_0 \int_0^t Z(\tau)d\tau}, \tag{30}$$

where

$$Z(t) = e^{-rI_0 \int_0^t e^{\left(r\int_0^\xi e^{w(\tau)}d\tau - \alpha\xi\right)}d\xi}. \tag{31}$$

Thus, we have proven the following:

Theorem 1. *If* $(S,\ I,\ R)$ *is a solution to the SIR epidemic model (1) and (3), then there are upper and lower bounds of the solution, such that we have*

$$S_1 \leq S \leq S_2,\ t \geq 0, \tag{32}$$

$$I_1 \leq I \leq I_2,\ t \geq 0 \tag{33}$$

and

$$R_1 \leq R \leq R_2,\ t \geq 0, \tag{34}$$

where

$$S_1 = e^w,\ \textit{where}\ w(t) = \left(\ln S_0 - \frac{c_1 + r}{\alpha - r}\right)e^{(r-\alpha)t} + \frac{c_1 + r}{\alpha - r}, \tag{35}$$

$$S_2 = S_0 e^{-rI_0 \int_0^t e^{\left(r\int_0^\xi e^{w(\tau)}d\tau - \alpha\xi\right)}d\xi}, \tag{36}$$

$$I_1 = I_0 e^{\left(r\int_0^t e^{w(\tau)}d\tau - \alpha t\right)}, \tag{37}$$

$$I_2 = I_0 e^{-\alpha t} e^{rS_0 \int_0^t Z(\tau)d\tau},\ Z(t) = e^{-rI_0 \int_0^t e^{\left(r\int_0^\xi e^{w(\tau)}d\tau - \alpha\xi\right)}d\xi}, \tag{38}$$

$$R_1 = \alpha \int_0^t I_1(\tau)d\tau \tag{39}$$

and

$$R_2 = \alpha \int_0^t I_2(\tau)d\tau, \tag{40}$$

2.2. Solutions in Parametric Forms

The following lemma is also an important tool in finding solutions in parametric forms to system (1)–(3).

Lemma 2. *System (6) can be also converted into an equivalent second-order nonlinear equation in v*

$$\frac{d^2v}{dt^2} = -r\left(\frac{dv}{dt} + \alpha\right)e^v. \tag{41}$$

Proof. Differentiating the second equation of (6) with respect to t, we obtain

$$\frac{d^2v}{dt^2} = r\frac{du}{dt}e^u. \tag{42}$$

We eliminate $\frac{du}{dt}$ and e^u from the right-hand side of (42) by using the first and second equations of (6), and we obtain (7).

Conversely, we can reduce Equation (41) to Equation (6) by setting the transformation $\frac{dv}{dt} = re^u - \alpha$, thus Equation (41) can be decoupled into

$$\begin{cases} \frac{dv}{dt} &= re^u - \alpha, \\ r\frac{du}{dt}e^u &= -r^2e^ve^u, \end{cases} \tag{43}$$

which is indeed (6), and this completes the proof. □

We rewrite Equation (41) as follows:

$$\frac{d^2(v+\alpha t)}{dt^2} = -re^{-\alpha t}\left(\frac{d(v+\alpha t)}{dt}\right)e^{v+\alpha t}. \tag{44}$$

Setting $w(t) = v + \alpha t$ gives

$$\frac{d^2w}{dt^2} = -re^{-\alpha t}\frac{dw}{dt}e^w. \tag{45}$$

The substitution $x = -\alpha t$ leads to

$$\frac{d^2w}{dx^2} = \frac{r}{\alpha}e^x\frac{dw}{dx}e^w. \tag{46}$$

Thus, the solution to this second-order nonlinear equation in the unknown $w(x)$ in parametric form is given by (Section 2.7.3-2 in [24]):

$$x = \int \frac{d\xi}{\xi f(\xi)} + d_2,\ w = \ln\left(\frac{\alpha f(\xi)}{r}\right) - \int \frac{d\xi}{\xi f(\xi)} - d_2. \tag{47}$$

where $f(\xi) = \xi + \ln \mid \xi \mid + d_1$ and $d_i,\ i = 1, 2$ are constants of integration.

We have the following:

Theorem 2. *The solution (S, I) in parametric form is given by*

$$t = -\frac{1}{\alpha}\int \frac{d\xi}{\xi f(\xi)} - \frac{d_2}{\alpha},\ S = \frac{\alpha}{r}f(\xi),\ I = -\frac{1}{r}\frac{d}{dt}\left[\ln(\frac{\alpha}{r}f(\xi))\right], \tag{48}$$

where $f(\xi) = \xi + \ln \mid \xi \mid + d_1$.

3. Analytic Approximate Solutions via Adomian Decomposition Method

We propose here to solve (5) using the Adomian decomposition method (ADM) [11–23].

First, we define the linear operator L, nonlinear operator N, and inverse linear operator L^{-1} as

$$L = \frac{d}{dt},\ N(u) = e^u,\ N(v) = e^v,\ L^{-1}(.) = \int_0^t (.)d\eta. \tag{49}$$

We rewrite (5) in Adomian's operator-theoretic notation as

$$\begin{cases} Lu &= -rN(v), \\ Lv &= -\alpha + rN(u). \end{cases} \tag{50}$$

Next, we apply L^{-1} to both sides of (50) as

$$\begin{cases} L^{-1}Lu &= -rL^{-1}[N(v)], \\ L^{-1}Lv &= -L^{-1}(\alpha) + rL^{-1}[N(u)], \end{cases} \tag{51}$$

where we calculate

$$L^{-1}Lu(t) = \int_0^t \frac{du}{d\tau}d\tau = u(t) - u(0),\ L^{-1}Lv(t) = \int_0^t \frac{dv}{d\tau}d\tau = v(t) - v(0). \tag{52}$$

Upon substitution, we have

$$\begin{cases} u(t) &= u(0) - rL^{-1}[N(v)], \\ v(t) &= v(0) - L^{-1}(\alpha) + rL^{-1}[N(u)]. \end{cases} \tag{53}$$

Using the classic Adomian decomposition method, we decompose the solution into the solution components to be determined via recursion and the nonlinearity into the corresponding Adomian polynomials tailored to the particular nonlinearity as

$$u(t) = \sum_{n=0}^{\infty} u_n(t),\ v(t) = \sum_{n=0}^{\infty} v_n(t),\ N(u) = \sum_{n=0}^{\infty} A_n(t),\ N(v) = \sum_{n=0}^{\infty} B_n(t), \tag{54}$$

where the first few Adomian polynomials [11,12] are given in the Appendix A.

Upon substitution, we obtain

$$\begin{cases} \sum_{n=0}^{\infty} u_n(t) &= u(0) - rL^{-1}[\sum_{n=0}^{\infty} B_n(t)], \\ \sum_{n=0}^{\infty} v_n(t) &= v(0) - L^{-1}(\alpha) + rL^{-1}[\sum_{n=0}^{\infty} A_n(t)]. \end{cases} \tag{55}$$

Then, we establish the Adomian recursion scheme as

$$\begin{cases} u_0(t) &= \ln S(0),\ v_0(t) = \ln I(0) - \alpha t, \\ u_{n+1}(t) &= -r\int_0^t B_n(\tau)d\tau,\ n \geq 0, \\ v_{n+1}(t) &= r\int_0^t A_n(\tau)d\tau,\ n \geq 0. \end{cases} \tag{56}$$

The first few components of the solution $(u,\ v)$ are given by

$$\begin{cases} u_0 &= \ln S(0), \\ u_1 &= \frac{rI(0)}{\alpha}(e^{-\alpha t} - 1), \\ u_2 &= \frac{r^2 I(0)S(0)}{\alpha^2}\left(\alpha t e^{-\alpha t} + e^{-\alpha t} - 1\right), \\ u_3 &= \frac{r^3 S(0)I(0)}{2\alpha^3}\Big(S(0)\left((\alpha^2 t^2 + 2\alpha t + 2)e^{\alpha t} - 2e^{2\alpha t}\right) + I(0)\left(\mathrm{e}^{2\alpha t} - 2\alpha t e^{\alpha t} - 1\right)\Big)\mathrm{e}^{-2\alpha t}, \\ &\cdots \end{cases} \tag{57}$$

$$\begin{cases} v_0 &= \ln I(0) - \alpha t, \\ v_1 &= rS(0)t, \\ v_2 &= -\frac{r^2 I(0)S(0)}{\alpha^2}\left(e^{-\alpha t} - 1 + \alpha t\right), \\ v_3 &= -\frac{r^3 S(0)I(0)}{4\alpha^3}\left(4S(0)\left(\alpha t\left(e^{-\alpha t}+1\right) + 2\left(e^{-\alpha t}-1\right)\right) + I(0)\left(e^{-2\alpha t} - 4e^{-\alpha t} - 2\alpha t + 3\right)\right) \\ &... \end{cases} \tag{58}$$

Hence,

$$S(t) = \exp(u_0 + u_1 + u_2 + u_3 + ...). \tag{59}$$

Attaining a satisfactory approximate solution for $S(t)$ will enable the determination of $I(t)$ and $R(t)$ using Equations (5) and (3), respectively. Notably, deriving from the second equation within system (5), we obtain

$$\frac{dv}{dt} = re^u - \alpha = rS - \alpha. \tag{60}$$

Integrating this equation from 0 to t, we obtain

$$v(t) - v(0) = r\int_0^t S(\tau)d\tau - \alpha t. \tag{61}$$

Then,

$$I(t) = I(0)e^{-\alpha t}e^{r\int_0^t S(\tau)d\tau}, \tag{62}$$

and

$$R(t) = \alpha\int_0^t I(\tau)d\tau. \tag{63}$$

It is important to note that when using the Adomian method, certain considerations must be taken into account. Indeed, the Adomian decomposition method is a precious tool for analyzing the SIR model, offering a systematic, analytical, and interpretable solution that significantly improves our understanding of infectious disease dynamics. It is imperative to thoroughly examine the convergence of the ADM series.

3.1. Convergence Analysis

3.1.1. Uniqueness Theorem

We can obtain a uniqueness theorem to this system beginning with the initial-value problem of Equation (7) with $u(0) = \ln S_0$.

Since $f(t,u) = re^u - \alpha u + c_1$ has $\frac{\partial f}{\partial u} = re^u - \alpha$, which is not bounded, f is not Lipschitzian. If we assume that there is a solution u to this initial-value problem which remains in $[0,b]$,, then, in the restricted region $(t,u) \in [0,\infty) \times [0,b]$, we have

$$f(t,u_1) - f(t,u_2) = r(e^{u_1} - e^{u_2}) - \alpha(u_1 - u_2) \text{ for all } u_1, u_2 \in [0,b]. \tag{64}$$

Applying the Mean Value Theorem to the function $r(e^{u_1} - e^{u_2})$, we obtain

$$f(t,u_1) - f(t,u_2) = (re^{u_*} - \alpha)(u_1 - u_2),\ u_1 \le u_* \le u_2. \tag{65}$$

Thus,

$$|\ f(t,u_1) - f(t,u_2)\ | \le |\ re^b - \alpha\ ||\ u_1 - u_2|. \tag{66}$$

Hence, $f(t,u)$ is Lipschitzian with $L_1 = |\ re^b - \alpha|$.

Assuming that u_1 and u_2 are two different solutions to this initial-value problem,

$$| \frac{d}{dt}(u_1 - u_2) | \leq L_1 | u_1 - u_2 | \text{ for all } u_1, u_2 \in [0, b]. \tag{67}$$

Using Gronwall's inequality, we obtain $| u_1 - u_2 | \leq 0$. Thus, $u_1 = u_2$.

Hence, the solution u to this initial-value problem exists and is unique. In view of this, we conclude that the solution (u, v) to (6) exists and is unique.

Consequently,

Theorem 3. *The SIR epidemic model has only one solution* $(S,\ I,\ R)$.

3.1.2. Convergence Theorem

The series solution obtained using the ADM converges with rapidity, and successive terms $(u_i,\ v_i)$ are easily computed. For the proof of the convergence of Adomian's method, we refer to the useful reference [25], in which Cherruault [25] proposed an interesting technique to prove the convergence under suitable and reasonable hypotheses for the numerical resolution of nonlinear equations. To examine this convergence, let us take the initial-value problem of Equation (7) with $u(0) = \ln S_0$, which is equivalent to the above system (50). For every convergent series $u(t) = \sum_{n=0}^{\infty} u_n(t)$, we define $N(u) = \sum_{n=0}^{\infty} A_n$, so that $N(\sum_{i=0}^{n} u_i(t)) = \sum_{i=0}^{n} A_i(u_0, u_1, ..., u_i)$.

The Adomian technique is equivalent to determine the sequences (U_n) [25]:

$$U_n = u_0 + u_1 + ... + u_n. \tag{68}$$

A simple computation leads to

$$A_n = N(U_n) - \sum_{i=0}^{n-1} A_i. \tag{69}$$

Let $\mathbb{X} = \mathbb{C}[0, T]$ be a Banach space of all continuous functions on $[0, T]$ with norm $\| u \|$, where $\| u \| = \max_{t\in[0,T]} | u |$. Consider the sequence of partial sums (U_n) with $n > m$. Thus,

$$\| U_n - U_m \| = \max_{t\in[0,T]} | U_n - U_m | = \max_{t\in[0,T]} | \sum_{i=m+1}^{n} u_i(t)|. \tag{70}$$

Hence,

$$\| U_n - U_m \| = \max_{t\in[0,T]} | \int_0^t \sum_{i=m}^{n-1} [-\alpha u_i(\tau) + r A_i(\tau)] d\tau|. \tag{71}$$

Use $\sum_{i=m}^{n-1} A_i = N(U_{n-1}) - N(U_{m-1})$ and $\sum_{i=m}^{n-1} u_i = U_{n-1} - U_{m-1}$ to get

$$\| U_n - U_m \| = \max_{t\in[0,T]} | \int_0^t [-\alpha(U_{n-1} - U_{m-1}) + r(N(U_{n-1}) - N(U_{m-1}))] d\tau|. \tag{72}$$

Since N is Lipschitzian with $L_1 = | re^b - \alpha |$,

$$\| U_n - U_m \| \leq L_1 T \| U_{n-1} - U_{m-1}||. \tag{73}$$

Similar arguments can be applied as in [26] to show that (U_n) is a Cauchy sequence in $\mathbb{X}$.

Thus,

Theorem 4. *The series solution* $u(t) = \sum_{n=0}^{\infty} u_n(t)$ *for the initial-value problem of Equation (7) with* $u(0) = \ln S_0$ *obtained via the ADM converging if* $0 < L_1 T < 1$ *and* $|u_1(t)| < \infty$.

4. Numerical Explorations and Analysis

In the beginning, we will investigate the numerical solutions to the SIR epidemic model (1) and (3) with the initial conditions (2) using the numerical solution using a Fehlberg fourth-fifth order Runge–Kutta method with a degree-four interpolant [27–30]. This method is also known as the Runge–Kutta–Fehlberg (RKF45) method and offers several advantages over traditional fixed-step methods like the standard fourth-order Runge–Kutta method. Indeed, solving ordinary differential equations using numerical methods is advantageous due to its adaptivity, higher accuracy, efficient error estimation, versatility, and widespread applicability.

In Figure 1, we present the numerical solutions to the SIR epidemic model (1) and (3) with the initial conditions (2). Left panel: $\alpha = 2., r = 1/5, I(0) = 25, S(0) = 75, R(0) = 0$. Mid panel: $\alpha = 2.73, r = 0.0178, I(0) = 7, S(0) = 254, R(0) = 0$. Right panel: $\alpha = 0.0164$, $r = 2.9236 \times 10^{-5}, I(0) = 2, S(0) = 4206, R(0) = 0$. These initial conditions and the values of the parameters of the system are well-chosen from [9,10], which are excellent cases with the SIR epidemic model.

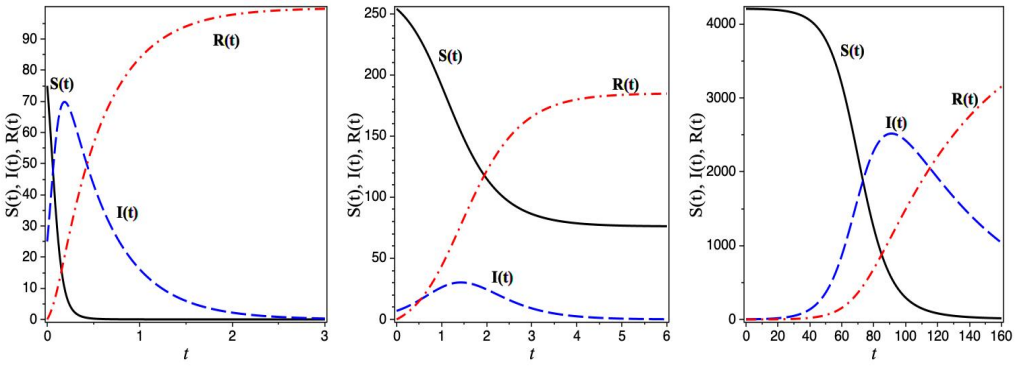

Figure 1. The numerical solutions to the SIR epidemic model (1) and (3) where the susceptible (S), infected (I), and recovered (R) populations are plotted versus time, with the initial conditions (2). (**Left panel**) $\alpha = 2., r = 1/5, I(0) = 25, S(0) = 75, R(0) = 0$ from [9]. (**Mid panel**) $\alpha = 2.73$, $r = 0.0178, I(0) = 7, S(0) = 254, R(0) = 0$ from [9]. (**Right panel**) $\alpha = 0.0164, r = 2.9236 \times 10^{-5}$, $I(0) = 2, S(0) = 4206, R(0) = 0$ from [10]. The representation is as follows: the solid black line corresponds to $S(t)$, the dashed blue line to $I(t)$, and the dash-dotted red line to $R(t)$. The solutions are in units of people and t is in months.

Here, we emphasize the essential point that is an essential property of the SIR model. The "positivity property" is a key concept in epidemiological modeling. It refers to the fact that variables like the number of individuals in different compartments, such as those who are susceptible, infected, or recovered, cannot be negative. This is because, in the context of infectious disease dynamics, it is impossible to have a negative number of individuals in any of these compartments. Therefore, the positivity property is an essential characteristic that must be considered when modeling the spread of infectious diseases.

Certainly, we observe from Equations (1)–(3) that $\frac{d}{dt}\big(S(t) + I(t) + R(t)\big) = 0$, establishing $S(t) + I(t) + R(t) = S(0) + I(0) + R(0) = N$, where N represents the total population. It can be straightforwardly demonstrated that $S(t) \geq 0$ and $I(t) \geq 0$ [2]. Furthermore, the essential characteristic is demonstrated in the numerical results illustrated in Figure 1.

Conversely, in Figure 2, we present the parametric solutions to the SIR epidemic model for the initial conditions $\alpha = 2, r = 1/5, I(0) = 25, S(0) = 75, R(0) = 0$. The parametric solutions to the SIR epidemic model offer several advantages in understanding and analyzing the dynamics of infectious diseases. In essence, parametric solutions to the SIR epidemic model facilitate a comprehensive understanding of infectious disease dynamics, providing insights into how different factors influence the spread and control of diseases and aiding in the development of effective public health strategies.

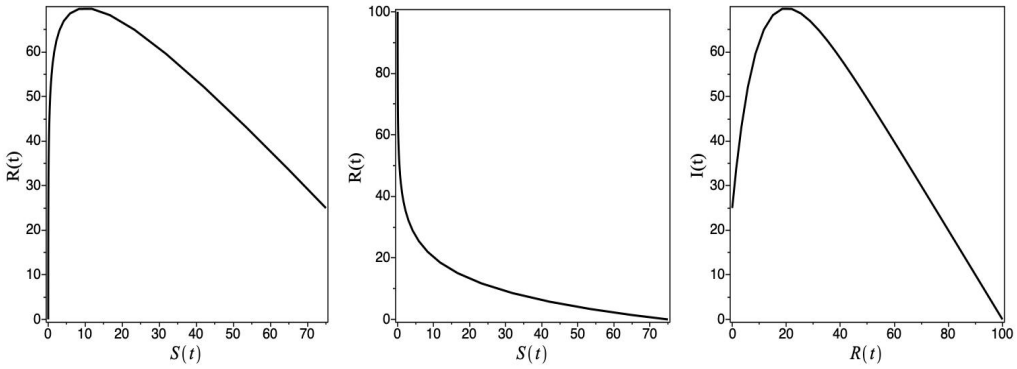

Figure 2. The parametric numerical solution to the SIR epidemic model (1) and (3) with the initial conditions (2). For the case $\alpha = 2, r = 1/5, I(0) = 25, S(0) = 75, R(0) = 0$ from [9].

In addition, to explore the finding of a good approximation for the SIR epidemic model, we suggest a useful, powerful technique that is called the Adomian decomposition method (ADM), which is used to solve nonlinear ordinary and partial differential equations. Its advantages lie in its simplicity, efficiency, and applicability to a wide range of nonlinear problems. However, the application of the ADM to the SIR epidemic model provides robust approximate solutions. Specifically, the method decomposes the nonlinear differential equations governing the dynamics of susceptible S, infected I, and recovered R populations into a series of functions. This decomposition enables the iterative solution of each constituent. In the context of the SIR model's nonlinear differential equations representing the changing rates of S, I, and R populations, ADM effectively breaks down these equations into a series of functions. This breakdown allows for the step-by-step determination of individual terms within the solution series. Meanwhile, it is essential to consider the reduction in numerical volume and the swift convergence of the approximate solutions for further progress. Our suggestion to employ the ADM technique that accounts for these factors is crucial for effective progress. The iterative process of the ADM involves computing Adomian polynomials and their associated coefficients. This computation method generates an approximate solution, which can be refined by including additional terms in the series expansion. Utilizing ADM facilitates the acquisition of an analytical approximation for the solution to the SIR epidemic model. This analytical approximation proves instrumental in comprehending disease dynamics, predicting its behavior under diverse conditions, and evaluating the effects of interventions or parameter variations on the transmission of infectious diseases.

In Figure 3, we present a comparison between the numerical solutions to the SIR epidemic model with the fourth order of the solutions that are obtained using the ADM techniques for the initial conditions $I(0) = 25, S(0) = 75, R(0) = 0$ with the parameters $\alpha = 2, r = 1/5$ [9,10]. The visual representation is delineated as follows: the dashed blue line depicts the numerical solution, the dotted black line illustrates the third-order solution derived using ADM, and the solid red line represents the fourth-order approximation attained through the ADM technique. The evident observation reveals a remarkable concurrence between the numerical solution and the fourth-order solutions obtained through the ADM technique for the function $S(t)$. There is appropriate agreement with numerical and fourth-order solutions by the ADM for the $I(t)$ and $R(t)$ functions.

In Figure 4, we present a comparison between the numerical solutions to the SIR epidemic model with the fifth order of the solutions that are obtained using the ADM techniques for the initial conditions $I(0) = 7, S(0) = 254, R(0) = 0$ with the parameters $\alpha = 2.73, r = 0.0178$, which involve a scenario studied by Khan et al. [9,10] to simulate the 1966 bubonic plague outbreak in Eyam, England [9,10]. The figure displays the numerical solution as solid lines and the fifth-order solution obtained using the ADM technique as dashed lines. S, I, and R correspond to the black, blue, and red lines, respectively. Upon careful observation, it is evident that there is a significant agreement between the

numerical solution and the fifth-order solutions obtained through the ADM technique for the functions at small values of t. For large values of t in months, numerical and fifth-order solutions obtained through the ADM for the functions have an appropriate agreement. The solutions are given in units of people. The right panel demonstrates a flawless alignment between the numerical solutions and the sixth-order solutions achieved through ADM. This highlights a significant advantage wherein ADM, even with lower orders of decomposition, can achieve remarkable agreement with the numerical solutions.

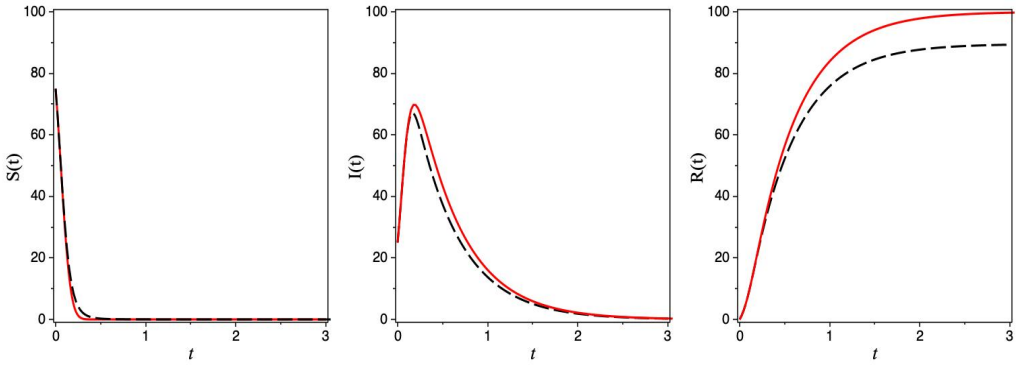

Figure 3. ADM and numerical solution to the SIR epidemic model (1) and (3) with the initial conditions (2). For the case $\alpha = 2, r = 1/5, I(0) = 25, S(0) = 75, R(0) = 0$ from [9]. The representation is as follows: the solid red line corresponds to the numerical solution, and the dashed black line is the fourth-order solution obtained using the ADM technique.

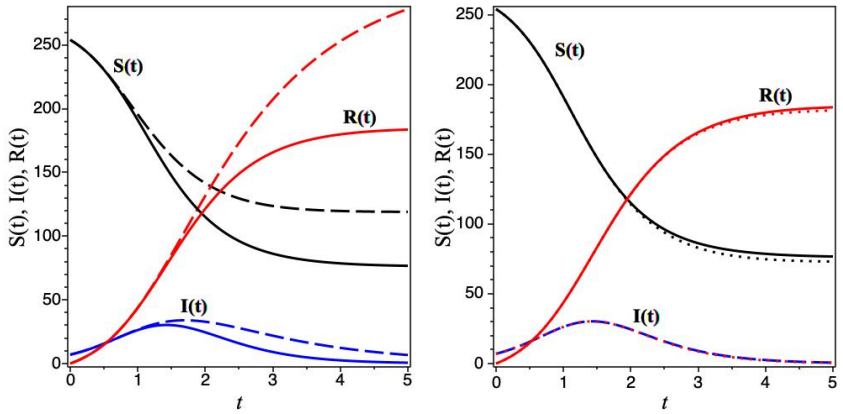

Figure 4. ADM and numerical solutions to the SIR epidemic model (1) and (3) with the initial conditions (2). For the case $\alpha = 2.73, r = 0.0178, I(0) = 7, S(0) = 254, R(0) = 0$ from [9]. (**Left panel**) The representation is as follows: the solid lines correspond to the numerical solution, and the dashed lines are the fifth-order solution obtained using the ADM technique. (**Right panel**) The dotted lines represent the sixth-order solution obtained using the ADM. Black line: S, blue lines: I, and red lines: R.

Figure 5 showcases a comparative analysis between the numerical solutions to the SIR epidemic model and the sixth-order solutions obtained using the ADM techniques. This evaluation pertains to specific initial conditions: $I(0) = 2, S(0) = 4206, R(0) = 0$, combined with the parameters $\alpha = 0.0164$ and $r = 2.9236 \times 10^{-5}$. In the left panel, a comparison between the seventh-order solutions obtained through the ADM and the numerical solutions reveals a notable discrepancy at larger time values, whereas, in the right panel, employing the eighth-order ADM solutions notably enhances the agreement. It should be noted that this scenario is a reference to a study conducted on the COVID-19 outbreak in Japan [10,31]. A slight increase in the order of decomposition in the ADM demonstrates improved concordance between numerical solutions and those derived via the ADM method. The ADM technique offers a valuable approach that delivers a strong approximation for the SIR epidemic model using lower-order decompositions, contrasting

with other methods necessitating higher-order series expansions [10]. By increasing the order of decomposition, we can effectively handle situations where both α and r are small. This approach ensures that we maintain the required level of accuracy in our results.

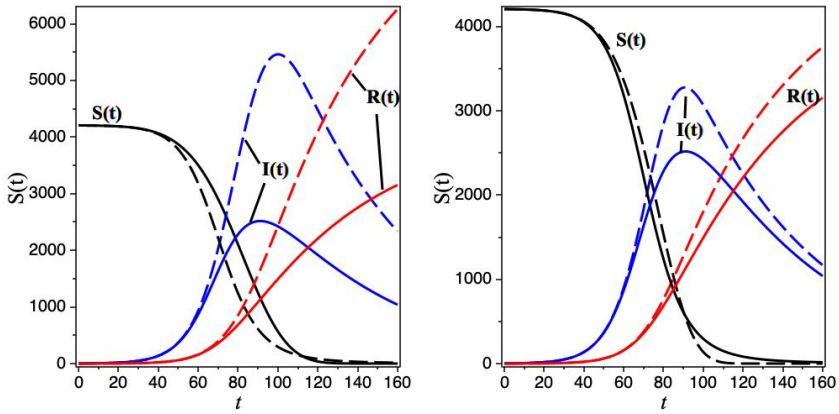

Figure 5. ADM and numerical solutions to the SIR epidemic model (1) and (3) with the initial conditions (2). For the case $\alpha = 0.0164, r = 2.9236 \times 10^{-5}, I(0) = 2, S(0) = 4206, R(0) = 0$ from Japan's COVID-19 outbreak data [10,31]. (**Left panel**) The representation is as follows: the solid lines correspond to the numerical solution, and the dashed lines are the seventh-order solution obtained using the ADM technique. (**Right panel**) The eighth-order solutions obtained using the ADM and the numerical solutions. Black line: S, blue lines: I, and red lines: R. Here, $t = 0$ is 22 January 2020 [10,31].

The proposed technique, which is directly stated, is said to offer a more efficient approach. This suggests that the proposed method can provide a solution of comparable quality while requiring fewer terms in the series expansion. This efficiency could have practical implications, such as reducing computational resources, simplifying calculations, or speeding up the modeling process. In essence, this point emphasizes the efficiency and effectiveness of the proposed technique in obtaining accurate solutions to the SIR model while streamlining the computational demands associated with other referenced methods [10]. On the other hand, the positive property persists in all the obtained results (Figures 3–5).

Further, by comparing the results obtained through the ADM with numerical solutions, we can gain valuable insights into the convergence behavior. If the ADM solutions closely match the numerical solutions for a variety of scenarios, it indicates that the convergence is favorable. This information can be instrumental in improving the accuracy and reliability of the ADM model.

The inclusion of additional terms in the series expansion can improve convergence. As we progressively refine the solution, we often assess the convergence behavior (Figures 4 and 5).

5. Conclusions

In conclusion, this research offers a comprehensive examination of the SIR epidemic model, delving into its meticulous formulation and employing innovative methodologies. The upper and lower bounds technique provides valuable insights into the interactions among susceptible, infected, and recovered populations and contributes to enhancing our theoretical comprehension through the derivation of an existence and uniqueness theorem. Moreover, applying the Adomian decomposition method demonstrates its effectiveness in yielding highly accurate approximate solutions to the SIR model.

Furthermore, the validation process, which involves numerical exploration across diverse experimental parameters, underscores the proposed approach's accuracy and robustness. This numerical analysis sheds light on the SIR model's sensitivity and adaptability under varying conditions, enriching our broader comprehension of infectious disease dynamics.

The suggested techniques explicitly highlight the useful efficiency, implying that it can provide an accurate satisfactory solution while utilizing fewer terms of the series expansion in the ADM method. This efficiency could have significant practical applications such as reducing the demand for computational resources, streamlining calculations, and expediting the modeling process.

This study has created a strong framework for studying the SIR model by combining theoretical formulation with numerical exploration. The findings of this study have significant implications for enhancing our predictive capabilities and improving strategies to manage and reduce the transmission of infectious diseases effectively.

Author Contributions: Conceptualization, L.B., S.B. and A.K.; methodology, L.B., A.K. and S.B.; software, S.B.; validation, L.B., A.K. and S.B.; formal analysis, A.K., L.B. and S.B.; investigation, A.K., L.B. and S.B.; writing original draft preparation, L.B., A.K. and S.B.; writing review and editing, A.K., L.B. and S.B. All authors have read and agreed to the published version of the manuscript.

Funding: This work was supported and funded by the Deanship of Scientific Research at Imam Mohammad Ibn Saud Islamic University (IMSIU) (grant number IMSIU-RG23018).

Institutional Review Board Statement: Not applicable.

Informed Consent Statement: Not applicable.

Data Availability Statement: This paper focuses on theoretical analysis and does not involve experiments and data.

Conflicts of Interest: The authors declare no conflicts of interest.

Appendix A. List of the Adomian Polynomials A_i for $N(u) = e^u$ [11–13]

$$
\begin{cases}
A_0 &= e^{u_0}, \\
A_1 &= u_1 e^{u_0}, \\
A_2 &= e^{u_0}\left[u_2 + \frac{1}{2}u_1^2\right], \\
A_3 &= e^{u_0}\left[u_3 + u_1u_2 + \frac{1}{6}u_1^3\right], \\
A_4 &= e^{u_0}\left[u_4 + (\frac{1}{2}u_2^2 + u_1u_3) + \frac{1}{2}u_1^2u_2 + \frac{1}{24}u_1^4\right], \\
A_5 &= e^{u_0}\left[u_5 + (u_2u_3 + u_1u_4) + \frac{1}{2!}(u_1u_2^2 + u_1^2u_3) + \frac{1}{3!}u_1^3u_2 + \frac{1}{5!}u_1^5\right], \\
A_6 &= e^{u_0}\left[u_6 + (u_1u_5 + u_2u_4 + \frac{1}{2!}u_3^2) + (\frac{1}{2!}u_1^2u_4 + u_1u_2u_3 + \frac{1}{3!}u_2^3) + (\frac{1}{3!}u_1^3u_3 + \frac{u_1^2u_2^2}{2!2!}) + \frac{1}{4!}u_1^4u_2 + \frac{1}{6!}u_1^6\right], \\
A_7 &= e^{u_0}\Big[u_7 + (u_3u_4 + u_2u_5 + u_1u_6) + (\frac{1}{2!}u_2^2u_3 + \frac{1}{2!}u_1u_3^2 + u_1u_2u_4 + \frac{1}{2!}u_1^2u_5) \\
&\quad + (\frac{1}{3!}u_1u_2^3 + \frac{1}{2!}u_1^2u_2u_3 + \frac{1}{3!}u_1^3u_4) + (\frac{1}{3!}\frac{1}{2!}u_1^3u_2^2 + \frac{1}{4!}u_1^4u_3) + \frac{1}{5!}u_1^5u_2 + \frac{1}{7!}u_1^7\Big], \\
A_8 &= e^{u_0}\Big[u_8 + (\frac{1}{2!}u_4^2 + u_3u_5 + u_2u_6 + u_1u_7) + (\frac{1}{2!}u_2u_3^2 + \frac{1}{2!}u_2^2u_4 + u_1u_3u_4 + u_1u_2u_5 \\
&\quad + \frac{1}{2!}u_1^2u_6) + (\frac{1}{4!}u_2^4 + \frac{1}{2!}u_1u_2^2u_3 + \frac{1}{2!}\frac{1}{2!}u_1^2u_3^2) + (\frac{1}{2!}u_1^2u_2u_4 + \frac{1}{3!}u_1^3u_5) \\
&\quad + (\frac{1}{2!}\frac{1}{3!}u_1^2u_2^3 + \frac{1}{3!}u_1^3u_2u_3 + \frac{1}{4!}u_1^4u_4) + (\frac{1}{4!}\frac{1}{2!}u_1^4u_2^2 + \frac{1}{5!}u_1^5u_3) + (\frac{1}{6!}u_1^6u_2 + \frac{1}{8!}u_1^8)\Big], \\
A_9 &= e^{u_0}\Big[u_9 + (u_4u_5 + u_3u_6 + u_2u_7 + u_1u_8) + (\frac{1}{3!}u_3^3 + u_2u_3u_4 + \frac{1}{2!}u_2^2u_5 + \frac{1}{2!}u_1u_4^2 \\
&\quad + u_1u_3u_5 + u_1u_2u_6 + \frac{1}{2!}u_1^2u_7) + (\frac{1}{3!}u_2^3u_3 + \frac{1}{2!}u_1u_2u_3^2 + \frac{1}{2!}u_1u_2^2u_4 + \frac{1}{2!}u_1^2u_3u_4 \\
&\quad + \frac{1}{2!}u_1^2u_2u_5 + \frac{1}{3!}u_1^3u_6) + (\frac{1}{4!}u_1u_2^4 + \frac{1}{2!}\frac{1}{2!}u_1^2u_2^2u_3 + \frac{1}{3!}\frac{1}{2!}u_1^3u_3^2 + \frac{1}{3!}u_1^3u_2u_4 + \frac{1}{4!}u_1^4u_5) \\
&\quad + (\frac{1}{3!}\frac{1}{3!}u_1^3u_2^3 + \frac{1}{4!}u_1^4u_2u_3 + \frac{1}{5!}u_1^5u_4 + \frac{1}{5!}\frac{1}{2!}u_1^5u_2^2 + \frac{1}{6!}u_1^6u_3 + \frac{1}{7!}u_1^7u_2 + \frac{1}{9!}u_1^9)\Big]. \\
&\ldots
\end{cases}
$$

The Adomian polynomials of B_i for $N(v) = e^v$ can be obtained in a similar form by using the functions v_i instead of u_i.

References

1. Kermack, W.O.; McKendrick, A.G. A contribution to the mathematical theory of epidemics. *Proc. R. Soc. Lond. Ser. A* **1927**, *115*, 700–721.
2. Bacaër, N. *A Short History of Mathematical Population Dynamics*; Springer: London, UK, 2011.
3. Yin, Z.; Yu, Y.; Lu, Z. Stability analysis of an age-structured SEIRS model with time delay. *Mathematics* **2020**, *8*, 455. [CrossRef]
4. Janssen, M.A.; Ostrom, E. Empirically based, agent-based models. *Ecol. Soc.* **2006**, *11*, 37. [CrossRef]
5. Mollalo, A.; Vahedi, B.; Rivera, K.M. GIS-based spatial modeling of COVID-19 incidence rate in the continental United States. *Sci. Total Environ.* **2020**, *728*, 138884. [CrossRef]
6. Sporns, O. Contributions and challenges for network models in cognitive neuroscience. *Nat. Neurosci.* **2014**, *17*, 652–660. [CrossRef] [PubMed]
7. Sun, J.; Chen, X.; Zhang, Z.; Lai, S.; Zhao, B.; Liu, H.; Wang, S.; Huan, W.; Zhao, R.; Ng, M.T.A.; et al. Forecasting the long-term trend of COVID-19 epidemic using a dynamic model. *Sci. Rep.* **2020**, *10*, 21122. [CrossRef]
8. Raval, M.; Sivashanmugam, P.; Pham, V.; Gohel, H.; Kaushik, A.; Wan, Y. Automated predictive analytics tool for rainfall forecasting. *Sci. Rep.* **2021**, *11*, 17704. [CrossRef] [PubMed]
9. Khan, H.; Mohapatra, R.N.; Vajravelu, K.; Liao, S.J. The explicit series solution of SIR and SIS epidemic models. *Appl. Math. Comput.* **2009**, *215*, 653. [CrossRef]
10. Barlow, N.S.; Weinstein, S.J. Accurate closed-form solution of the SIR epidemic model. *Physica D* **2020**, *408*, 132540; Erratum in *Physica D* **2021**, *416*, 132807. [CrossRef] [PubMed]
11. Adomian, G. *Solving Frontier Problems of Physics: The Decomposition Method*; Kluwer Academic: Dordrecht, The Netherlands, 1994.
12. Adomian, G. Modification of decomposition approach to the heat equation. *J. Math. Anal. Appl.* **1987**, *124*, 290–291. [CrossRef]
13. Adomian, G.; Rach, R.C. Inhomogeneous nonlinear partial differential equations with variable coefficients. *Appl. Math. Lett.* **1992**, *5*, 11–12. [CrossRef]
14. Adomian, G.; Rach, R.C. Analytic solution of nonlinear boundary-value problems in several dimensions by decomposition. *J. Math. Anal. Appl.* **1993**, *174*, 118–137. [CrossRef]
15. Duan, J.-S.; Rach, R. A new modification of the Adomian decomposition method for solving boundary value problems for higher order differential equations. *Appl. Math. Comput.* **2011**, *218*, 4090–4118. [CrossRef]
16. Duan, J.-S.; Rach, R.; Wazwaz, A.-M. Solution of the model of beam-type micro- and nano-scale electrostatic actuators by a new modified Adomian decomposition method for nonlinear boundary value problems. *Int. J. Non-Linear Mech.* **2013**, *49*, 159–169. [CrossRef]
17. Duan, J.-S.; Rach, R.; Wazwaz, A.-M.; Chaolu, T.; Wang, Z. A new modified Adomian decomposition method and its multistage form for solving nonlinear boundary value problems with Robin boundary conditions. *Appl. Math. Modell.* **2013**, *37*, 8687–8708. [CrossRef]
18. Duan, J.-S.; Rach, R.; Wazwaz, A.-M. A reliable algorithm for positive solutions of nonlinear boundary value problems by the multistage Adomian decomposition method. *Open Eng.* **2014**, *5*, 59–74. [CrossRef]
19. Wazwaz, A.-M. *Partial Differential Equations and Solitary Waves Theory*; Higher Education Press: Beijing, China; Springer: Berlin/Heidelberg, Germany, 2009.
20. Bougoffa, L.; Rach, R.C.; El-Manouni, S. A convergence analysis of the Adomian decomposition method for an abstract Cauchy problem of a system of first-order nonlinear differential equations. *Int. J. Comput. Math.* **2013**, *90*, 360–375. [CrossRef]
21. Bougoffa, L.; Rach, R.C.; Wazwaz, A.M.; Duan, J.S. On the Adomian decomposition method for solving the Stefan problem. *Int. J. Numer. Methods Heat Fluid Flow* **2015**, *25*, 912–928. [CrossRef]
22. Bougoffa, L.; Bougouffa, S. Adomian method for solving some coupled systems of two equations. *Appl. Math. Comput.* **2006**, *177*, 553–560. [CrossRef]
23. Bougoffa, L.; Bougouffa, S. Solutions of the two-wave interactions in quadratic nonlinear media. *Mathematics* **2020**, *8*, 1867. [CrossRef]
24. Polyanin, A.D.; Zaitsev, V.F. *Handbook of Exact Solutions for Ordinary Differential Equations*, 2nd ed.; Chapman and Hall/CRC: Boca Raton, FL, USA, 2003.
25. Cherruault, Y. Convergence of Adomian's method. *Math. Comput. Model.* **1990**, *14*, 83–86. [CrossRef]
26. El-Kalla, I.L. Convergence of the Adomian method applied to a class of nonlinear integral equations. *Appl. Math. Lett.* **2008**, *21*, 372–376. [CrossRef]
27. Enright, W.H.; Jackson, K.R.; Norsett, S.P.; Thomsen, P.G. Interpolants for Runge-Kutta Formulas. *ACM Trans. Math. Softw.* **1986**, *12*, 193–218. [CrossRef]
28. Fehlberg, E. Klassische Runge-Kutta-Formeln vierter und niedrigerer Ordnung mit Schrittweiten-Kontrolle und ihre Anwendung auf Waermeleitungsprobleme. *Computing* **1970**, *6*, 61–71. [CrossRef]
29. Forsythe, G.E.; Malcolm, M.A.; Moler, C.B. *Computer Methods for Mathematical Computations*; Prentice Hall: Hoboken, NJ, USA, 1977.

30. Shampine, F.L.; Corless, M.R. Initial Value Problems for ODEs in Problem-Solving Environments. *J. Comp. Appl. Math.* **2000**, *125*, 31–40. [CrossRef]
31. John Hopkins University. CSSE Novel Coronavirus (COVID-19) Cases. Available online: https://github.com/CSSEGISandData/COVID-19 (accessed on 10 March 2023).